[K. Maki and T. Tsuneto, Progr. Theoret. Phys. (Kyoto) 31, 945 (1964)], the difference of carrier number density of electrons and holes in the theory of antiferromagnetic chromium by T. M. Rice, Phys. Rev. B 2, 3619 (1970), or that in the theory of excitonic instability under strong magnetic fields in Bi by H. Fukuyama and T. Nagai, Phys. Rev. B 3, 4413 (1971); J. Phys. Soc. Japan 31, 812 (1971).

[21]M. Saitoh, H. Fukuyama, H. Shiba, and Y. Uemura, J. Phys. Soc. Japan 27, 26 (1969).

[22]H. Fukuyama, M. Saitoh, H. Siba, and Y. Uemura, J. Phys. Soc. Japan 28, 842 (1970); H. Siba, K. Kanda, H. Hasegawa, and H. Fukuyama, *ibid.* 30, 972 (1971).

[23]P. Fulde and A. Luther, Phys. Rev. 170, 570 (1968).

PHYSICAL REVIEW B VOLUME 5, NUMBER 8 15 APRIL 1972

Lattice Dynamics of Noble Metals—Application to Copper

Satya Prakash
Physics Department, Punjabi University, Patiala, India

and

S. K. Joshi
Physics Department, University of Roorkee, Roorkee, India

(Received 7 July 1971)

A model band structure with noninteracting s and d bands for copper is used to calculate the static dielectric function and the phonon frequencies. A local empirical pseudopotential is used to describe the electron-ion matrix element for both the s and d electrons. The exchange and the correlation effects are completely neglected. The calculated phonon frequencies are found in fair agreement with the experimental measurements for the longitudinal branches, while the agreement is poor for the transverse branches. It is inferred that the itinerant nature of the d electrons should not be overlooked in a calculation of phonon frequencies of noble metals.

I. INTRODUCTION

A decade ago Toya studied the lattice dynamics of copper, [1] but the method he used was exactly the same as the one he had used for the alkali metals. The free-electron wave function and the parabolic energy bands were utilized to calculate the electron-phonon interaction. Toya emphasized the importance of core overlap effects in a calculation of phonon frequencies of copper. He used the Born-Mayer exchange overlap potential, treated the potential parameters as adjustable, and obtained them by fitting the phonon frequencies for the longitudinal and the transverse modes at the zone boundary in the [111] direction to the values measured by Jacobsen[2] using the diffuse x-ray scattering method. Sinha[3] compared his experimental neutron-diffraction measurements with the frequencies calculated on the basis of Toya's model with a few minor modifications. He obtained the parameters introduced in the electron-ion matrix element and in the Born-Mayer exchange overlap potential by requiring that the phonon frequencies in the long-wavelength limit agree with those derived from the measured values of elastic constants. The phonon frequencies calculated by him were found to be in good quantitative agreement with experimental results. Srivastava and Dayal[4] have calculated the dispersion curves for copper using a variant of Toya's approach. They used the same parameters that Toya had used. The difference was that they used Bailyn's[5] results for the electron-ion matrix element and the effect of exchange and correlations in the screening. The detailed band-structure calculations[6–9] of copper clearly show that there is an overlap between s and d bands. The d electrons are not explicitly considered in Toya's model, except that they are incorporated in the core and the core-core-overlap interaction is represented by a phenomenological potential.

Golibersuch[10] and Sinha[11] have discussed the electron-phonon interaction using the augmented-plane-wave method. Sinha's treatment is based on the assumption that each core may be regarded as carrying along with it in the course of displacements due to lattice vibrations a portion of valence charge density which may be thought as rigidly bound to the core. The first-order-perturbed charge density may then be split up into a bound part and a deformable part. The bound part results into a weak residual ionic potential. A self-consistent equation is set up for the deformable part and this leads to a self-consistent response to the weak residual potential. This method seems to be quite suitable for noble metals. Because the method involves very involved and complicated calculations, it has not been applied to any metal as yet.

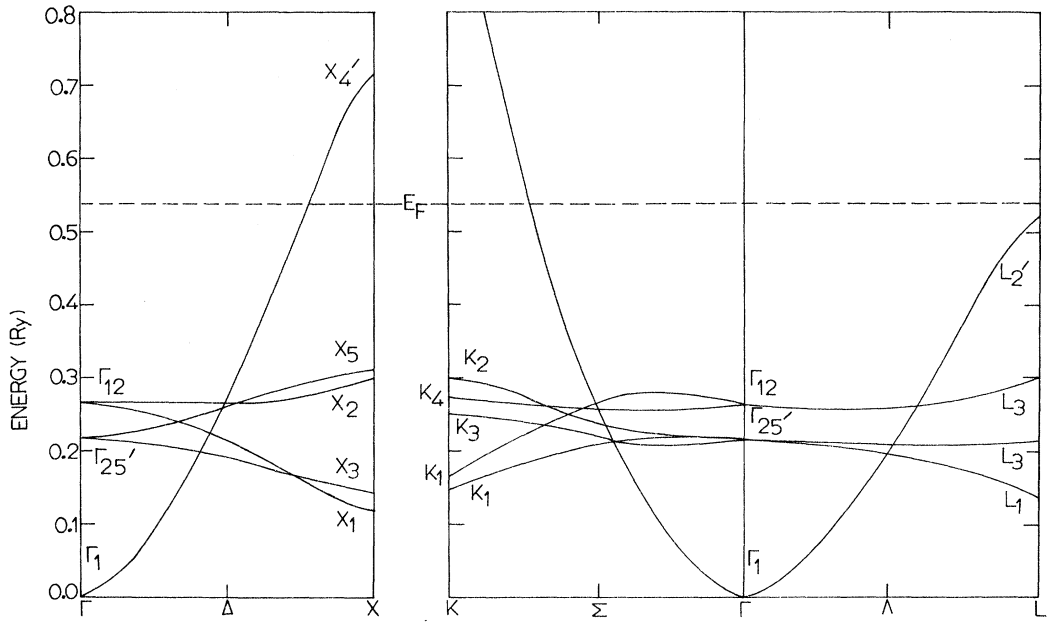

FIG. 1. Model for the noninteracting bands for copper based on the calculations of Snow and Waber (Ref. 8). Dashed line shows the Fermi energy.

Ziman,[12] Harrison,[13] and Deegan[14] have proposed extensions of the pseudopotential concept for the d-band metals. So far the pseudopotential approach has not been applied to study the lattice dynamics of noble metals.

Recently we proposed a noninteracting band model for the dielectric screening in transition metals[15] (hereafter this paper is referred to as I) and applied it to calculate the phonon frequencies of paramagnetic nickel[16] (hereafter this paper is referred to as II). In these calculations we neglected the off-diagonal part of the dielectric matrix.[17] A fairly satisfactory agreement between the calculated and the measured phonon frequencies was obtained. The model used by us for the paramagnetic transition metals should also be applicable to noble metals. We have applied this model here to calculate the phonon frequencies of copper. Several detailed band-structure calculations and the experimental measurements for phonon frequencies[18] are available for copper. Relativistic effects are not as important for copper as they are for other noble metals.

TABLE I. m assignments to different d subbands.

[010]	[110]	[111]	m
$\Gamma_{12}\rightarrow X_2$	$\Gamma_{12}\rightarrow K_4$	$\Gamma_{12}\rightarrow L_3$	2
$\Gamma_{12}\rightarrow X_1$	$\Gamma_{12}\rightarrow K_1$	$\Gamma_{12}\rightarrow L_3$	0
$\Gamma_{25'}\rightarrow X_5$	$\Gamma_{25'}\rightarrow K_2$	$\Gamma_{25'}\rightarrow L_3$	1
$\Gamma_{25'}\rightarrow X_3$	$\Gamma_{25'}\rightarrow K_3$	$\Gamma_{25'}\rightarrow L_3$	−1
$\Gamma_{25'}\rightarrow X_3$	$\Gamma_{25'}\rightarrow K_1$	$\Gamma_{25'}\rightarrow L_1$	−2

In Sec. II we describe the model band structure of copper and use it in Sec. III to calculate the static dielectric function. The calculation of phonon dispersion relations is presented in Sec. IV and the results are discussed in Sec. V.

II. MODEL BAND STRUCTURE

We choose the recent band-structure calculations of Snow and Waber[8] to construct a noninteracting band model. They used the self-consistent augmented-plane-wave scheme in their calculation. The s and d characters of the wave function in the band vary as we change the electron wave vector $\vec{k}$ in the zone. The bands have dominantly s character at Γ_1, but d character dominates at X, L,

TABLE II. Physical parameters of copper.

Lattice constant a_l (in Bohr units a_0)	6.8309
Volume of the unit cell Ω_0 (in a_0^3 units)	79.6835
Radius of the Brillouin sphere K_B (in $1/a_0$ units)	0.9057
Fermi momentum for the s band K_{Fs} (in $1/a_0$ units)	0.7189
Effective mass for the s band m_s (in a.u.)	0.9603
Number of s electrons per atom Z_s	1

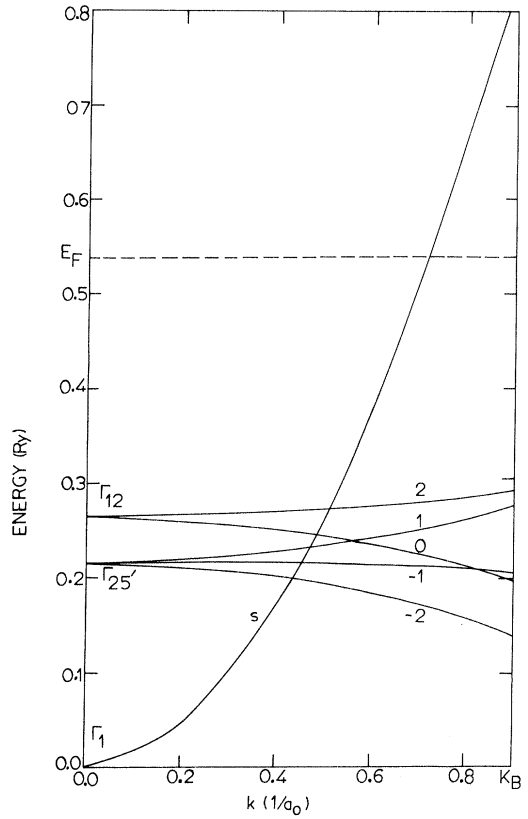

FIG. 2. Isotropic energy-band structure for copper. The numbers near the curves for the d subbands denote the magnetic quantum number m assigned to them.

and K symmetry points.

We consider only the electron dispersion relations along the three principal symmetry directions [010], [110], and [111]. As explained in I, the s bands are obtained by joining Γ_1 to X_4, and Γ_1 to K_1 (not shown in the Fig. 1), respectively. For d bands, Γ_{12} is joined to X_1 in the [010] direction, Γ_{12} and $\Gamma_{25'}$ are joined with upper and lower K_1, respectively, in the [110] direction, and $\Gamma_{25'}$ is joined with L_1 in the [111] direction. The noninteracting bands obtained in this manner are shown in the Fig. 1, where the origin of energy is shifted to Γ_1. Here and later, the energy is measured in rydbergs and the distances are measured in units of the Bohr radius.

The d band are fivefold degenerate and the different d subbands should be assigned different magnetic quantum numbers m. This is done exactly in the manner described in I. The assignments of m for different d subbands along three principal symmetry directions are given in Table I. It is evident from the Fig. 1 that the Fermi level intersects only the s band. The d subbands are sufficiently below the Fermi level and are therefore completely filled with two electrons per atom. The effective mass for the s band is calculated with the help of the relation

$$m_s = \hbar^2 k_{Fs}^2 / 2E_F \,, \tag{1}$$

TABLE III. Average effective masses for d subbands (in a.u.).

m	0	1	−1	2	−2
m_{dm}	−12.3584	14.4326	−83.5384	31.8953	−10.7558

TABLE IV. Parameters for $3d$ radial wave function.

i	1	2	3	4
a_i	1.4105	23.0751	125.4921	79.6966
α_i	1.5370	3.0624	5.7817	10.3718

TABLE V. Relative magnitudes of $\epsilon_{ss}(\vec{p})$ and $\epsilon_{ds}(\vec{p})$ for copper. Here p is in units of $1/a_0$.

$\lvert\vec{p}\rvert$	$-\epsilon_{ss}(p)$	$-\epsilon_{ds}(p)$
	[100] direction	
0.1	87.7222	72.4816
0.2	21.8237	18.5101
0.4	5.3474	4.9320
0.6	2.2935	2.1955
0.8	1.2209	0.9622
1.0	0.7191	0.4392
1.5	0.1631	0.0765
2.0	0.0429	0.0235
2.5	0.0167	0.0095
3.0	0.0079	0.0046
3.5	0.0045	0.0021
4.0	0.0024	0.0014
4.5	0.0015	0.0009
5.0	0.0009	0.0005
	[110] direction	
0.1414	43.7900	39.4736
0.2828	10.8401	10.4411
0.5657	2.5992	2.8873
0.8485	1.0668	0.9132
1.1314	0.5197	0.2957
2.1213	0.0334	0.0202
2.8284	0.0100	0.0063
3.5355	0.0040	0.0026
4.2426	0.0019	0.0012
4.9498	0.0010	0.0007
	[111] direction	
0.1732	29.1458	27.2446
0.3464	7.1785	7.4359
0.6928	1.6814	1.7964
1.0392	0.6521	0.1228
1.7321	0.0812	0.0479
2.5981	0.0142	0.0091
3.4641	0.0044	0.0029
4.3301	0.0018	0.0012
5.1962	0.0008	0.0006

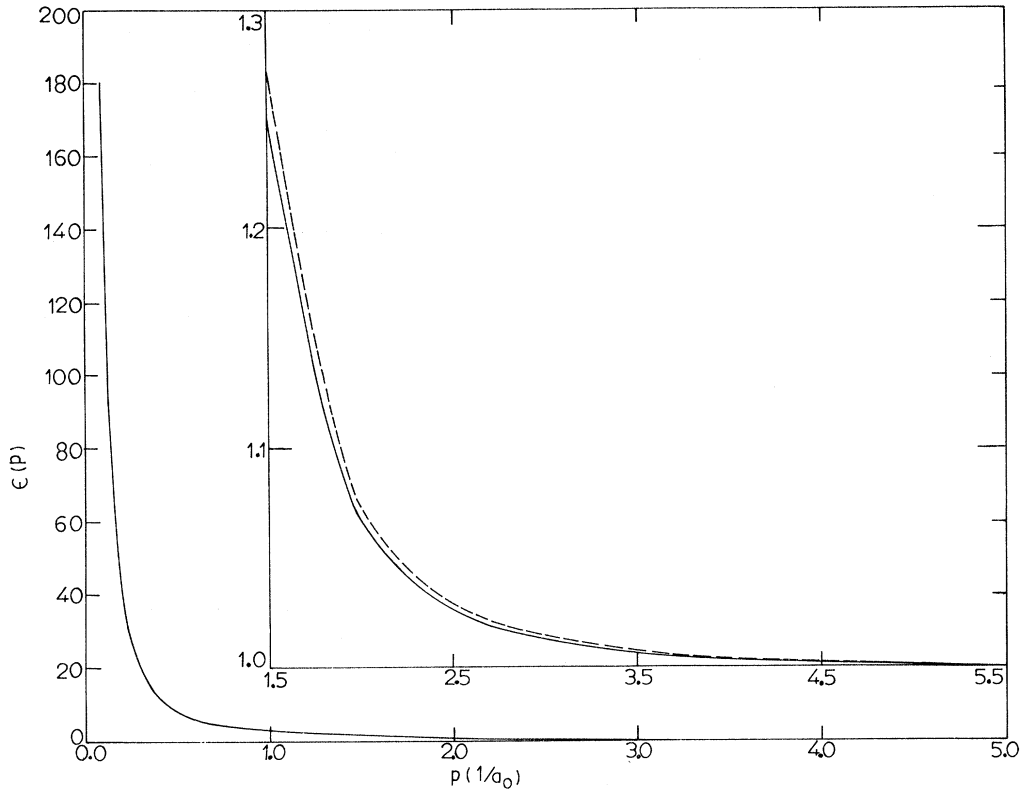

FIG. 3. $\epsilon(\vec{p})$ vs $\vec{p}$ for copper. $\epsilon(\vec{p})$ is represented by a solid line along the [100] direction. In the present scale, the values of $\epsilon(\vec{p})$ along the [110] and [111] directions coincide with the solid line. In the upper right-hand corner $\epsilon(\vec{p})$ is plotted on a magnified scale for $p > 1.5$. The dashed line represents the dielectric function calculated by Eq. (16). For $p < 1.25$ the dashed line almost coincides with solid line.

where E_F is the Fermi energy and

$$k_{Fs} = (3\pi^2 Z_s/\Omega_0)^{1/3} . \tag{2}$$

Z_s is the number of s electrons per atom and Ω_0 is the volume of the unit cell. The average effective masses for different d subbands are calculated in the same manner as described in I. The physical parameters for copper are tabulated in Table II and the average effective masses m_{dm} are presented in Table III. The model isotropic energy-band structure obtained with the help of average effective masses is shown in Fig. 2.

III. DIELECTRIC FUNCTION

In the model band structure that we have taken for copper, the d subbands are completely filled. Each filled d subband accommodates two electrons. The readjustment of the electrons in response to the displacement of ions due to the lattice vibrations will be caused by the following two types of transitions: (i) from unfilled s band to unfilled s band and (ii) from filled d subbands to unfilled s band. Therefore the dielectric function is written in the form

$$\epsilon(\vec{p}) = 1 - \epsilon_{ss}(\vec{p}) - \epsilon_{ds}(\vec{p}) . \tag{3}$$

ϵ_{ss} and ϵ_{ds} represent the contributions from s-to-s and d-to-s transitions, respectively. $\vec{p} = \vec{q} + \vec{G}$, where $\vec{q}$ is the phonon wave vector and $\vec{G}$ is the reciprocal-lattice vector. Here we shall only reproduce the formulas for ϵ_{ss} and ϵ_{ds} which are derived in I:

$$\epsilon_{ss}(\vec{p}) = -\frac{2m_s k_{Fs} e^2}{\pi\hbar^2 p^2}\left(1 + \frac{4k_{Fs}^2 - p^2}{4k_{Fs}p} \ln\left|\frac{2k_{Fs}+p}{2k_{Fs}-p}\right|\right) \tag{4}$$

and

$$\epsilon_{ds}(\vec{p}) = \frac{32e^2}{\Omega_0 p^2}\frac{m_s}{\hbar^2}\sum_m (-1)^m \Bigg(\int_0^{k_{Fdm}} dk\, k^2 [F_2(k)]^2 \times [D_{0m}^2 D_{0-m}^2 I_0 + (D_{1m}^2 D_{-1-m}^2 + D_{-1m}^2 D_{1-m}^2) I_1 + (D_{2m}^2 D_{-2-m}^2 + D_{-2m}^2 D_{2-m}^2) I_2] \Bigg) . \tag{5}$$

$D_{m'm}^2$ are the elements of the rotation matrices with argument $(-\gamma, -\beta, -\alpha)$ where α, β, γ are the Euler's angles and

$$k_{Fdm} = (3\pi^2 Z_{dm}/\Omega_0)^{1/3} , \tag{6}$$

$$I_0 = \tfrac{5}{4}\ (\tfrac{1}{2} I_{n0} - 3 I_{n2} + \tfrac{9}{2} I_{n4}) ,$$

$$I_1 = \tfrac{15}{4}\ (-I_{n2} + I_{n4}) , \tag{7}$$

$$I_2 = \tfrac{15}{8}\ (\tfrac{1}{2} I_{n0} - I_{n2} + \tfrac{1}{2} I_{n4}) ,$$

where

$$I_{n0} = -\frac{1}{b} \ln\left|\frac{b-a}{b+a}\right| ,$$

$$I_{n2} = -\frac{1}{b}\left(\frac{2a}{b} + \frac{a^2}{b^2} \ln\left|\frac{b-a}{b+a}\right|\right) , \tag{8}$$

$$I_{n4} = -\frac{1}{b}\left(\frac{2a}{3b} + \frac{2a^3}{b^3} + \frac{a^4}{b^4} \ln\left|\frac{b-a}{b+a}\right|\right) ,$$

$$a = k^2(m_s/m_{dm} - 1) - p^2 , \tag{9}$$

$$b = 2kp , \tag{10}$$

$$F_2(k) = 48k^2 \sum_i \frac{a_i \alpha_i}{(\alpha_i + k^2)^4} . \tag{11}$$

Z_{dn} is the number of electrons per atom in the mth d subband and a_i and α_i are the parameters of the $3d$ radial wave function

$$R_{3d}(r) = \sum_{i=1}^{4} a_i r^2 e^{-\alpha_i r} . \tag{12}$$

We use the neutral-atom $3d$ radial wave function due to Watson[19] for the atomic configuration $3d^{10}4s^1$. The parameters a_i and α_i are tabulated in the Table IV.

$\epsilon_{ss}(\vec{p})$ and $\epsilon_{ds}(\vec{p})$ are calculated with the help of Eqs. (4) and (5). $\epsilon_{ss}(\vec{p})$ depends on the magnitude of $\vec{p}$ only, while $\epsilon_{ds}(\vec{p})$ depends on the direction of $\vec{p}$ also. The procedure described in I is adopted to calculate $\epsilon_{ds}(\vec{p})$ along the three principal symmetry directions [010], [110], and [111]. $\epsilon_{ss}(\vec{p})$ and $\epsilon_{ds}(\vec{p})$ are tabulated in Table V along all the three principal symmetry directions for a set of values of $\vec{p}$. $\epsilon(\vec{p})$ is shown as a function of $\vec{p}$ along all the three symmetry directions in Fig. 3. The dielectric function has an almost isotropic behavior. $\epsilon_{ss}(\vec{p})$ and $\epsilon_{ds}(\vec{p})$ are of the same order of magnitude in all the three directions for copper, while $\epsilon_{ds}(\vec{p})$ was negligible in comparison to $\epsilon_{ss}(\vec{p})$ in the case of paramagnetic nickel.

IV. LATTICE DYNAMICS

The method of calculating the electronic contribution $\omega^2_{qp}(E)$ to the square of the phonon frequencies is given in II. The final expression obtained in II for $\omega^2_{qp}(E)$ is

$$\omega^2_{qp}(E) = -\omega^2_{pl}\left(\sum_G \frac{\{\vec{e}_{qp}\cdot(\vec{q}+\vec{G})\}^2}{|\vec{q}+\vec{G}|^2} F(\vec{q}+\vec{G})\right.$$

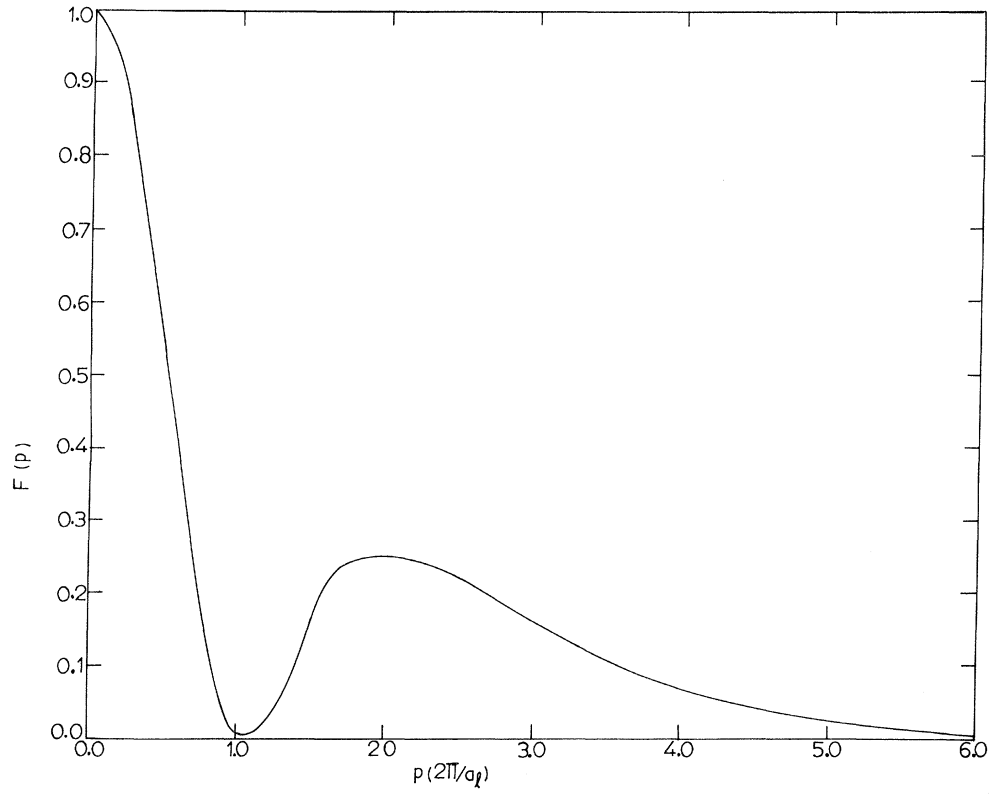

FIG. 4. Function $F(p)$ vs p for copper.

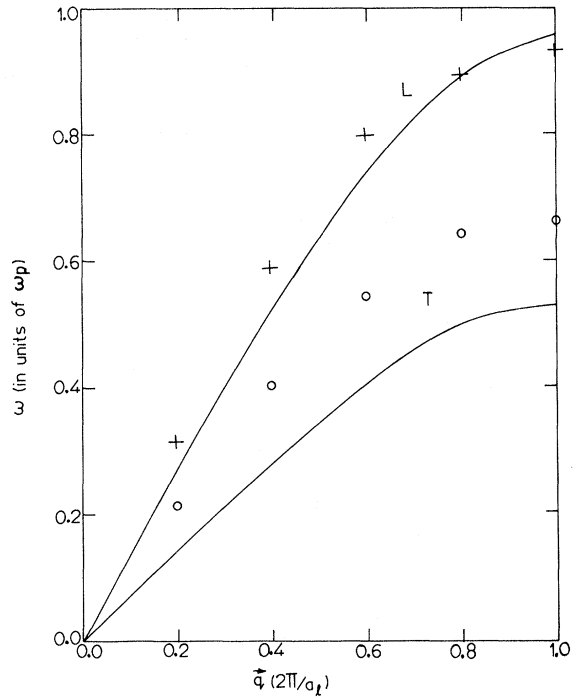

FIG. 5. ω vs $\vec{q}$ for copper along the [100] direction. + denotes the experimental phonon frequency for the longitudinal branch; ○ represents the transverse branch.

$$-\sum_{\vec{G}\neq 0}\frac{\{\vec{e}_{qp}\cdot\vec{G}\}^2}{|\vec{G}|^2}F(\vec{G})\Bigg)\,, \tag{13}$$

where

$$F(p)=\left(1-\frac{1}{\epsilon(p)}\right)\left(-1+\frac{p^2}{4\pi z e^2}\,\frac{\beta'}{[1+(pr_c)^2]^2}\right)^2 \tag{14}$$

and

$$\omega_{pl}^2=4\pi z^2e^2/m\Omega_0\,. \tag{15}$$

$\vec{e}_{pq}$ is the unit polarization vector for the phonon wave vector $\vec{q}$ and the polarization branch $\vec{p}$, and z is the effective ionic charge. M is the ionic mass, and β' and r_c are two parameters of the model pseudopotential which is used for the bare-ion potential.[16] The contribution to the phonon frequencies due to Coulombic interaction between the ions is evaluated by Ewald's[20] method and have been tabulated by Vosko *et al.*[21] for an fcc lattice along the three principal symmetry directions [100], [110], and [111]. We have neglected the contribution to phonon frequencies due to overlap potential between the ions. The effective ionic charge is taken to be unity, assuming that the electrons lying in the filled bands are bound to the nuclei, and therefore the core is limited to $3d^{10}$ configuration. The deform-

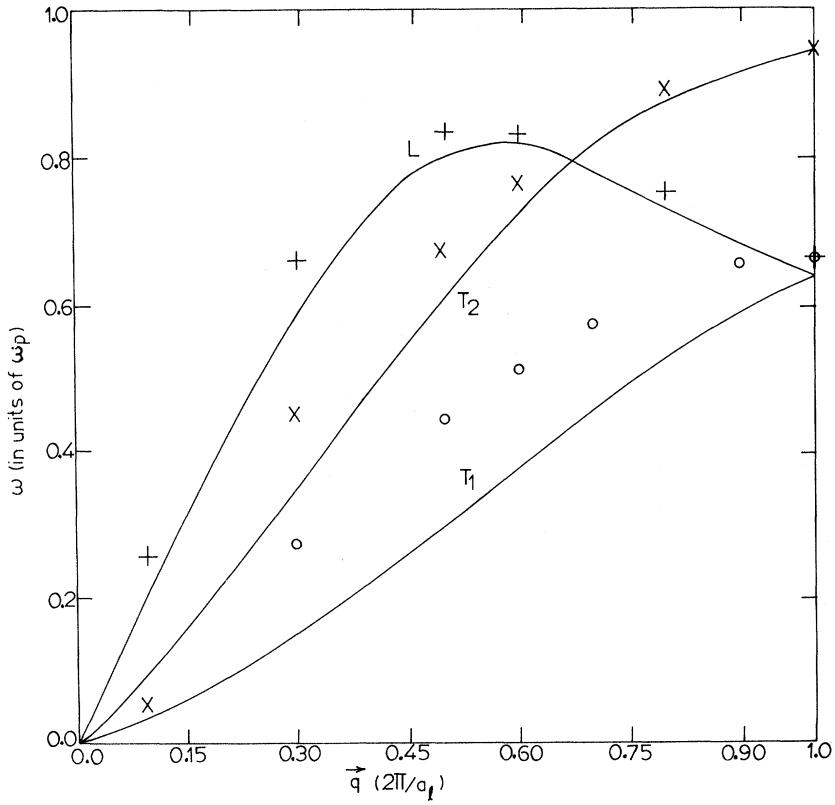

FIG. 6. ω vs $\vec{q}$ for copper along the [110] direction. The description of the figure is the same as that of Fig. 4, except that × represents an experimental phonon frequency of the T_2 branch, while ○ represents an experimental phonon frequency of the T_1 branch.

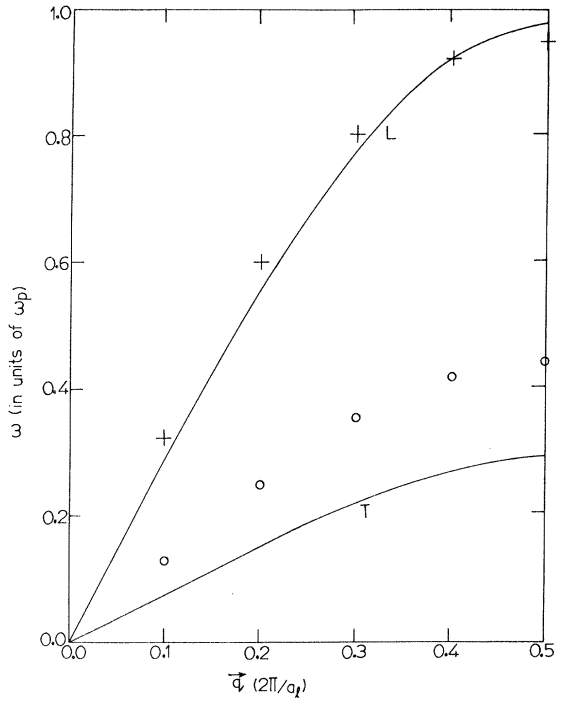

FIG. 7. ω vs $\vec{q}$ for copper along the [111] direction. The description of the figure is the same as that of Fig. 4.

ability of this core is approximately considered through ϵ_{ds}.

We cannot neglect $\epsilon_{ds}(\vec{p})$ as we could in II for nickel. It is beyond our computational efforts to evaluate the complete $\vec{k}$-dependent dielectric function and to use it to calculate the phonon frequencies for a set of phonon wave vectors. Therefore we thought of another scheme. We represented $\epsilon_{ds}(\vec{p})$ by an analytic function of the same form as for $\epsilon_{ss}(\vec{p})$, but therein we treat k_d as a variable parameter:

$$\epsilon(\vec{p}) = 1 + \frac{2m_s k_{Fs} e^2}{\pi\hbar^2 p^2}\left(1 + \frac{4k_{Fs}^2 - p^2}{4k_{Fs}p}\ln\left|\frac{2k_{Fs}+p}{2k_{Fs}-p}\right|\right) + \frac{2m_s k_d e^2}{\pi\hbar^2 p^2}\left(1 + \frac{4k_d^2 - p^2}{4k_d p}\ln\left|\frac{2k_d+p}{2k_d-p}\right|\right) . \quad (16)$$

For $k_d = 0.6384$, the values calculated on the basis of this function are found to be in close agreement with the values based on the detailed calculation of ϵ_{ds} discussed above.

The phonon frequencies of copper are calculated in the same manner as described in II with the help of Eqs. (13) and (16). The variable parameters β' and r_c are adjusted to achieve an agreement with the experimental measurements in the longitudinal branch in the [100] direction at the zone boundary. We found that for $\beta' = 14.4$ and $r_c = 0.25$, the calculated phonon frequencies are in satisfactory agreement for $q = 1.0$ in the longitudinal branch of [100] direction. Using these values for β' and r_c, the phonon frequencies were calculated for the symmetry directions [100], [110], and [111] for the longitudinal and the transverse branches. The sum over $\vec{G}$ in (13) is taken for 259 nearest-reciprocal-lattice vectors, where the function $F(\vec{p})$ converges properly as shown in Fig. 4. The calculated phonon frequencies are compared with the experimental measurements in the Figs. 5–7 along the symmetry directions. The phonon frequencies in the longitudinal branches and T_2 branch in the [110] direction are in satisfactory agreement with the experimental measurements, but the phonon frequencies in the transverse branches are as low as 30% for some wave vectors. If we use the bare-ion potential calculated by the modified Hartree-Fock-Slater[22,23] scheme, we face the same difficulties as we did in the case of paramagnetic nickel discussed in II.

V. DISCUSSION

The model that we have used is too simplified a picture of a noble metal. Though the noninteracting band model is based on the detailed band-structure calculations, we did not consider explicitly the s-d hybridization which splits s and d bands. We neglected the exchange and correlation effects, which should be quite important. The core limited to $3d^{10}$ configuration should overlap with nearest neighbors, but we have neglected the contribution of overlap potential. We have incorporated in this model the effect of mutual orthogonalization of s- and d-electron wave functions and their orthogonalization to the core wave functions in a phenomenological way. A local empirical model potential is used for the bare-ion potential. This may not be too bad an approximation for the s electrons, but it is certainly a poor approximation for the d electrons. A rigorous formulation will result in a very complicated form for the dielectric function.

ACKNOWLEDGMENTS

The authors acknowledge financial support from the Department of Atomic Energy, Government of India. One of us (SP) also thanks Professor B. S. Sood for encouragement.

[1] T. Toya, J. Res. Inst. Catalysis Hokkaido Univ. 9, 178 (1961); Progr. Theoret. Phys. (Kyoto) 20, 974 (1958).
[2] E. H. Jacobsen, Phys. Rev. 97, 654 (1955).
[3] S. K. Sinha, Phys. Rev. 143, 422 (1966).
[4] P. L. Srivastava and B. Dayal, Phys. Rev. 140, A1014 (1965).
[5] M. Bailyn, Phys. Rev. 117, 974 (1960).
[6] G. A. Burdick, Phys. Rev. 129, 138 (1963).

[7]B. Segall, Phys. Rev. 125, 109 (1962).
[8]E. C. Snow and J. T. Waber, Phys. Rev. 157, 570 (1967).
[9]J. S. Faulkner, H. L. Davis, and H. W. Joy, Phys. Rev. 161, 656 (1967); 167, 601 (1968).
[10]D. C. Golibersuch, Phys. Rev. 157, 532 (1967).
[11]S. K. Sinha, Phys. Rev. 169, 477 (1968).
[12]J. M. Ziman, Proc. Phys. Soc. (London) 86, 237 (1965).
[13]W. A. Harrison, Phys. Rev. 181, 1036 (1969).
[14]R. A. Deegan, Phys. Rev. 186, 619 (1969).
[15]S. Prakash and S. K. Joshi, Phys. Rev. B 2, 915 (1970).
[16]S. Prakash and S. K. Joshi, Phys. Rev. B 4, 1770 (1971).
[17]S. Prakash and S. K. Joshi, Phys. Rev. B3, 1512 (1971).
[18]R. M. Nicklow, G. Gilat, H. G. Smith, L. J. Raubenheimer, and M. K. Wilkinson, Phys. Rev. 164, 922 (1967).
[19]R. E. Watson, MIT Solid State and Molecular Theory Group Technical Report No. 12, 1958 (unpublished).
[20]E. W. Kellerman, Phil. Trans. Roy. Soc. London A238, 513 (1940).
[21]S. H. Vosko, R. Taylor, and G. H. Keech, Can. J. Phys. 43, 1187 (1965).
[22]S. Prakash and S. K. Joshi, Phys. Rev. 187, 808 (1969).
[23]S. Prakash and S. K. Joshi, Phys. Letters 30A, 138 (1969).

PHYSICAL REVIEW B VOLUME 5, NUMBER 8 15 APRIL 1972

Optimum-Model-Potential Lattice Dynamics of β-Sn†

Z. Kam*
Department of Physics, Technion-Israel Institute of Technology, Haifa, Israel

and

G. Gilat‡
IBM Research Laboratories, Monterey & Cottle Roads, San Jose, California
(Received 22 July 1971)

Shaw and Harrison's optimized form of the model potential of Heine, Abarenkov, and Animalu has been employed for the calculation of energy wave-number characteristics and phonon dispersion relations in β-Sn. A good fit with experimental dispersion relations can be obtained by using the electron effective mass m^* as a free parameter with the value $m^*=1.4$. For this value of m^*, the calculated dispersion relations display a certain fine structure which is observed experimentally. The quality of fit of the model to experimental data depends sensitively on m^*. It is also deduced that, unless m^* is suitably adjusted, Shaw's method of including exchange and correlation in the model potential does not produce low enough phonon frequencies in the case of β-Sn. Nonlocal contributions to the model potential play a significant role in accounting for phonon data. This model is also employed to calculate $g(\omega)$, which is compared with data of coherent scattering of neutrons from polycrystalline β-Sn.

I. INTRODUCTION

The pseudopotential approach for the theory of simple metals has become very popular and has proved successful in many applications. In a recent review by Heine, Cohen, and Weaire[1] the state of art in this field has been brought up to date and summarized. The reader is referred to this review for a complete account of the subject and many references.

Of all measurable metallic properties, one that gives any theory a serious challenge is the phonon spectrum $\omega_j(\vec{q})$. This challenge is manifested by the large number of individual observations that theory must account for. From general experience gathered so far, it is concluded that the amount of difficulty encountered in the actual application of the pseudopotential method increases with the number of conduction electrons per atom, with the number of core electrons, and with the lowering of crystal symmetry. For instance, in order to obtain the same quality of fit between theoretical and experimental phonon data, it is necessary to raise the sophistication and complexity of the theoretical model in going, for example, from sodium to magnesium to zinc.

The main source of difficulty in calculating phonon dispersion relations arises from the high degree of cancellation between the ionic (Coulomb) and the electronic contributions to the phonon dynamical matrix. In some cases, especially for low-energy phonons, the difference between these two contributions may amount only to a few percent of their respective values. Here, the phonon energy $\hbar\omega(\vec{q})$ becomes an extremely sensitive quantity which changes appreciably for small adjustments in the theory. The pseudopotential theory is therefore likely to be more successful with less